Journal of Biotechnology 336 (2021) 1–9

Contents lists available at ScienceDirect

Journal of Biotechnology

journal homepage: www.elsevier.com/locate/jbiotec

Host nutrition-based approach for biotechnological production of the antifungal cyclic lipopeptide jagaricin

Nicolas Schlosser [a,c], Jordi Espino-Martínez [a], Florian Kloss [b], Florian Meyer [b], Bettina Bardl [a], Miriam A. Rosenbaum [a,c], Lars Regestein [a,*]

[a] Bio Pilot Plant, Leibniz Institute for Natural Product Research and Infection Biology, Hans Knoell Institute, Adolf-Reichwein-Str. 23, 07745, Jena, Germany
[b] Transfer Group Anti-Infectives, Leibniz Institute for Natural Product Research and Infection Biology, Hans Knoell Institute, Adolf-Reichwein-Str. 23, 07745, Jena, Germany
[c] Faculty of Biological Sciences, Friedrich Schiller University Jena, 07745, Jena, Germany

ARTICLE INFO

Keywords:
Antifungal
Mushroom
Agaricus bisporus
Antimicrobial
Cyclic lipopeptide

ABSTRACT

In today's, society multi-resistant pathogens have become an emerging threat, which makes the search for novel anti-infectives more urgent than ever. A promising class of substances are cyclic lipopeptides like the antifungal jagaricin. Jagaricin is formed by the bacterial mushroom pathogen *Janthinobacterium agaricidamnosum*. It has shown antifungal activity against human pathogenic fungi like *Candida albicans* and *Aspergillus fumigatus*. In addition, jagaricin is nearly non-toxic for plants, which makes it a promising agent for agricultural applications. Cyclic lipopeptides formed by microorganisms originate from their secondary metabolism. This makes it very challenging to determine the inducing factor for product formation, especially for unknown microbial systems like *J. agaricidamnosum*. In the presented study, a biotechnological process for jagaricin formation was developed, investigating impact factors like the medium, oxygen availability, and phosphate. For this reason, experiments were conducted on microtiter plate, shake flask, and stirred tank bioreactor level. Ultimately, a final maximum jagaricin concentration of 251 mg L^{-1} (15.5 $mg_{Jagaricin} \cdot g_{CDW}^{-1}$) could be achieved, which is an increase of approximately 458 % in comparison to previous results in standard glucose medium. This concentration allows the production of significantly higher amounts of jagaricin and enables further experiments to investigate the potential of this substance.

1. Introduction

Antimicrobial resistant microbes like drug-resistant Candida, methicillin-resistant *Staphylococcus aureus* (MRSA), or azole-resistant *Aspergillus fumigatus* have become a serious threat to our today's society (CDC, 2019). Health agencies around the world have been drawing attention to this threat for decades. In the United States of America, about 2.8 million infections and more than 35.000 deaths caused by antimicrobial resistant bacteria and fungi are recorded each year (CDC, 2019; WHO, 2017). This makes the search for and the development of new drugs with novel mechanisms of action more urgent than ever. A promising class of natural products hereby are cyclic lipopeptides.

Cyclic lipopeptides (CLP) are amphiphilic molecules consisting of a hydrophilic peptide head group linked to a fatty acid tail (Hamley, 2015). Well-known microbial producers are strains of *Pseudomonas*, *Bacillus*, and *Streptomyces* (Coutte et al., 2017; Mnif and Ghribi, 2015). CLPs have shown antibacterial (Meena and Kanwar, 2015), antiviral (Wang et al., 2017), antifungal (Fischer et al., 2019; Gonzalez-Jaramillo et al., 2017) as well as antitumoral activities (Chauhan and Kanwar, 2020; Duarte et al., 2014). For example, micafungin (Mycamine®) and caspofungin (Cancidas®), both belong to the antifungal class of echinocandins, are already approved drugs used in the treatment of invasive candidiasis and *Aspergillus* infections, respectively (Cross and Scott, 2008; Morrison, 2005). Another well-known but antibacterial CLP is daptomycin (Cubicin®), It is one of the last reserve antibiotics used in the treatment of skin and soft tissue infections caused by Gram-positives (Kornberger et al., 2016; Taylor and Palmer, 2016).

Due to the high antimicrobial potential of CLPs in general, new representatives of this group are of interest. Jagaricin is produced by the Gram-negative, aerobic bacterium *Janthinobacterium agaricidamnosum,*

* Corresponding author at: Leibniz Institute for Natural Product Research and Infection Biology, Hans Knoell Institute, Adolf-Reichwein-Str. 23, 07745, Jena, Germany.
E-mail address: lars.regestein@leibniz-hki.de (L. Regestein).

https://doi.org/10.1016/j.jbiotec.2021.06.015
Received 3 March 2021; Received in revised form 26 May 2021; Accepted 7 June 2021
Available online 9 June 2021

which is known for causing soft rot disease in the cultivated mushroom *Agaricus bisporus* (Lincoln et al., 1999; Pudełko, 2013). This new CLP was discovered by Graupner et al. (2012) as a key virulence factor involved in the soft rot pathogenesis. It was also shown that its activity also applies to human pathogenic fungi like *Candida albicans*, *Aspergillus fumigatus,* and *Aspergillus terreus* and that it acts by impairing the membrane integrity through the formation of pores, through which even calcium ions can diffuse into fungal cells. Additionally, it was figured out that jagaricin also acts against phytopathogenic fungi like *Alternaria alternata*, *Penicillium digitatum*, and *Fusarium graminearum*, whereas it does not inhibit germination of plant model hosts (*Sinapis alba* and *Lepidium sativum*) within the tested range. Thus, jagaricin could be relevant for agricultural applications (Fischer et al., 2019; Ines and Dhouha, 2015). Although the genome of *J. agaricidamnosum* is completely analysed and the *jag* gene locus, coding e.g. nonribosomal peptide synthetase (NRPS) modules, discovered (Graupner et al., 2015), the molecular trigger inducing jagaricin formation is not yet deciphered. To investigate the full potential of jagaricin in proof of concept studies as well as for the chemical conversion into new derivatives, however, the results from early laboratory research need to be transferred into a scalable well-characterized process to generate relevant amounts.

In the past years, multiple approaches to seize this challenge were developed, but these approaches are specific for each process. For surfactin as an example, a well-known CLP produced by *Bacillus subtilis* (Raaijmakers et al., 2010), several potential impact factors are known to affect the product formation. Besides temperature and pH, which may influence nearly every metabolic pathway, the availability of oxygen seems to play an important role (Sen and Swaminathan, 1997; Shaligram and Singhal, 2010; Yao et al., 2015). Furthermore, the most critical and important parameters are the nutrients provided through the medium (Rangarajan and Clarke, 2015). Macronutrients like the carbon source, nitrogen, and phosphate have a huge impact on cell growth and also on product formation. Especially, phosphate limitation is a very well-known way to trigger the formation of many secondary metabolites (Martin, 2004; Singh et al., 2016). Also the presence or limitation of micronutrients and trace elements can serve as a trigger for the formation of secondary metabolites. Hereby, iron and manganese play an important role in biosurfactants production (Chen et al., 2015; Weinberg, 1969, 1990).

Lipopeptides can provide their producers a broad variety of advantageous biological functions. For example, they can make insoluble nutrients more accessible for the pathogen by lowering the surface tension (Geudens and Martins, 2018; Götze and Stallforth, 2019; Raaijmakers et al., 2010). For *J. agaricidamnosum* – *A. bisporus* interaction, it was assumed that *A. bisporus* is a nutritionally valuable source. The mushroom is rich in proteins, vitamins (B-group), trace elements like iron and potassium, and phosphorus (Muszyńska et al., 2017; Reis et al., 2012). A further hypothesis is that jagaricin is not only a virulence factor but supports also cell wall degrading enzymes (e.g. chitinoclastic activity) during the infection process of *A. bisporus* (Graupner et al., 2012; Haack et al., 2016). The hydrolyzed polysaccharides are the main carbon source in this environment.

Based on the existing microbiological knowledge of the *J. agaricidamnosum* – *A. bisporus* interaction, this study aims at increasing the biotechnological accessibility of jagaricin by choosing host related carbon sources as well as trace elements based on the mushroom composition. Moreover, considering for previously reported successes to generate the cyclic lipopeptides surfactin, iturin, and fengycin, the impact of phosphate and oxygen availability was elucidated. The outcome lays an important foundation for subsequent evaluations of the potential of jagaricin as a bioactive compound and its biotechnological accessibility.

2. Materials and methods

2.1. Microbial strain

In this study, a wild-type strain of *Janthinobacterium agaricidamnosum* DSM 9628 (DSMZ, Braunschweig, Germany) was used. The working cell bank was stored at −80 °C in a 1:1 mixture (v/v) of culture broth with glycerol conservation medium. The glycerol conservation medium contained in g L^{-1}: K_2HPO_4, 12.6; Na-citrate, 0.9; $MgSO_4 \times 7\ H_2O$, 0.18; $(NH_4)_2SO_4$, 1.8; KH_2PO_4, 3.6; glycerol, 88.

2.2. Media

All experiments were conducted in a complex medium containing: 10 g L^{-1} yeast extract (OHLY GmbH, Hamburg, Germany) and 5 g L^{-1} Na-L-glutamate (Sigma-Aldrich Chemie GmbH, Munich, Germany). The trace element solution was prepared as a stock solution that contained in g L^{-1}: $CaCl_2 \times 2\ H_2O$, 1; iron(III) citrate $\times\ H_2O$, 0.2; $MnSO_4$, 0.1; $ZnCl_2$, 0.03; $CoCl_2 \times 6\ H_2O$, 0.04; $CuSO_4 \times 5\ H_2O$, 0.03; $Na_2MoO_4 \times 2\ H_2O$, 0.06; $Na_2B_4O_7 \times 10\ H_2O$. In microtiter plate screenings $CaCl_2 \times 2\ H_2O$ (Sigma-Aldrich, Germany), as well as trace element solution were added in different concentrations as stated in the legend of the respective figure. The carbon sources (glucose, mannose, sucrose, fructose, and mannitol) were prepared as stock solutions, sterilized by filtration (0.2 µm PES Steriflip-GP filtration unit, Merck, Germany), and added with the indicated concentrations.

2.3. Pre-culture

Prior to inoculation of the main cultures in microtiter-, shake flask or 7-L stirred tank bioreactor scale, a two-staged pre-culture was prepared. The complex medium (DSMZ medium 605 receipt) for both pre-culture steps contained per L (Fischer et al., 2019): 1 g beef extract (Becton Dickinson GmbH, Heidelberg, Germany); 2 g yeast extract (OHLY GmbH, Hamburg, Germany); 5 g bacto™ peptone (Becton Dickinson GmbH, Heidelberg, Germany); 5 g NaCl (Carl Roth GmbH, Karlsruhe, Germany). Before sterilization at 121 °C and 1 bar overpressure for 20 min, pH was adjusted to 6.5 with 4 M NaOH. A 500 mL Erlenmeyer flask with a filling volume of 30 mL complex medium was inoculated from the cryostock (1 mL). The pre-culture was incubated on an orbital shaker (ISF1-X, Adolf Kühner AG, Birsfelden, Switzerland) with a shaking diameter of 50 mm and shaking frequency of 200 rpm at 25 °C till an OD_{600} of 0.5 was reached. The second pre-culture was inoculated with an initial OD_{600} of 0.1 in a 2 L Erlenmeyer flask with a filling volume of 150 mL and incubated for 8 h.

2.4. Microtiter plate experiments

All experiments in microtiter plates were conducted in 48 round well microtiter plates (m2p-labs GmbH, Baesweiler, Germany) using the BioLector® (m2p-labs GmbH, Baesweiler, Germany) cultivation system (Funke et al., 2010; Wewetzer et al., 2015). The shaking diameter of the orbital shaker was set to 3 mm. To ensure oxygen unlimited conditions, the maximum oxygen transfer rate (OTR_{max}) was calculated before culturing according to an equation published by Lattermann et al. (2014). With a shaking frequency of 1.000 rpm, a filling volume of 1 mL, as well as the geometric parameters of a round well plate, the OTR_{max} has a value of 39 mmol L^{-1} h^{-1}. The initial OD_{600} was 0.1. To limit evaporation, the microtiter plates were foil-sealed with F-GPR48-10 (m2p-labs GmbH, Baesweiler, Germany) and the incubation chamber was humidified with water at 85 %. The biomass growth was measured by scattered light at a gain of 25. All microtiter plate experiments were buffered with 50 mM MOPS (3-morpholinopropane-1-sulfonic acid). The initial pH was adjusted to 6.5 with 4 M NaOH.

2.5. Shake flask experiments

The impact of the oxygen supply on jagaricin production was investigated in shake flask cultivations using the TOM® system (Adolf Kühner AG, Birsfelden, Switzerland). for online measurement of carbon dioxide formation and oxygen uptake (Anderlei and Büchs, 2001; Anderlei et al., 2004; Büchs, 2001) installed in an orbital shaker (ISF1-X, Adolf Kühner AG, Birsfelden, Switzerland). Cultivations were performed in 250 mL shake flasks and a shaking diameter of 50 mm. Shaking frequencies and filling volumes were modified as stated in the captions. The initial OD_{600} was 0.1. Additionally, three non-monitored shake flasks for each cultivation condition were run in parallel for harvesting and creation of offline samples at specific events.

2.6. Stirred tank bioreactor

Fermentations were performed in batch mode using a baffled 7-L stirred tank bioreactor (Biostat B-DCU II, Sartorius Biotech, Germany) equipped with 6-bladed dual Rushton turbines. The filling volume was 4 L in all cases. To avoid foaming, which is a major challenge in the production of biosurfactants (Blesken et al., 2020), the polypropylene-based Antifoam 204 (Sigma-Aldrich, Munich, Germany) was used, if necessary. The aeration of the bioreactor was adjusted to 0.5 vvm. The stirring rate was increased to maintain the dissolved oxygen tension (DOT) at $\geq$20 %. The initial OD_{600} was 0.1. Except for the scale-up experiment, the pH was controlled by the addition of different bases and acids as stated in the captions of the figures and regulated in a tight range (6.50 $\pm$ 0.05).

2.7. Offline analytics

The biomass in shake flask and stirred tank bioreactor cultivations was determined gravimetrically as cell dry weight (CDW). Three pre-weighed 2 mL tubes per sample were filled with 2 mL of culture broth each and centrifuged for 10 min at 16.000 RCF (Micro centrifuge 5415 C, Eppendorf, Germany). The biomass pellet was dried in a drying oven at 60 °C for at least 48 h (until weight constancy) and weighted with an analytical balance (XS205DU, Mettler Toledo, Gießen, Germany). The supernatant was separated and used for the analytics of metabolites, carbon sources, nitrogen, and phosphate. Nitrogen was quantified by the Kjeldahl titration method using the AutoKjeldahl unit K-370 (Büchi, Flawil, Switzerland). Phosphate was quantified spectrophotometrically using a phosphate test kit (PMB, Merck) and the Spectroquant®NOVA 60. Glucose was measured with the glucose analyzer 2900D (YSI, Yellow springs OH, USA). Other sugars (fructose, mannose, sucrose) and sugar alcohol (mannitol) were chromatographically analysed by HPLC (JASCO International Co, Tokyo, Japan). A Rezex RCM Monosaccharide column (300 mm × 7.8 mm, 8 µm, Phenomenex, Torrance CA, USA) was used for separation. The instrument was operated isocratically with water as mobile phase at a flow rate of 0.5 mL min^{-1} and an oven temperature of 80 °C. Refractive index (RI) was used for detection. Amino acids were analysed by UHPLC (JASCO International Co, Tokyo, Japan). Precolumn derivatization was conducted with o-phthaldialdehyde reagent using a SecurityGuard Ultra Cartridge column (Phenomenex, Torrance CA, USA). A Kinetex XB C18 Column (75 mm x 2.1 mm, 2.6 µm, Phenomenex, Torrance CA, USA) was used for subsequent separation. The instrument was operated with 20 mM potassium phosphate (A) at pH 7.2 and (B) acetonitrile-methanol 50:50 (v/v). The flow rate was 0.25 mL min^{-1} and the oven temperature was set to 25 °C. The initial gradient of 10 % B was held for 1 min, then increased to 60 % B after 25 min and decreased again to 10 % B after 28 min. Quantification was achieved by fluorescence detection (excitation 340 nm, emission 455 nm).

2.8. Jagaricin extraction and analytics

For the quantification of jagaricin, samples were initially modified via organic solvent extraction (Biniarz and Lukaszewicz, 2017). Culture broth samples (500 µL) were extracted with 1.5 mL of methanol (HiPerSolv CHROMANORM, VWR Chemicals). Extracts were vortexed for 10 s and centrifuged at 16.000 RCF. Supernatants were used for the analytics. Analytical runs were performed on UHPLC system (Thermo Fisher Scientific, Waltham MA, USA) equipped with a diode array detector. A Kinetex XB-C18 column (100 mm x 2.1 mm, 1.7 µm, Phenomenex, Torrance CA, USA) was used for separation. The instrument was operated with 0.1 % trifluoroacetic acid (TFA) in water (A) and 0.1 % TFA in ACN (B) at a flow rate of 0.4 mL min^{-1}. The initial percentage of 5 % B was held for 1 min, was then linearly increased to 98 % B within 4 min and held for another 3 min before it was set to the starting conditions. Jagaricin was detected at 254 nm. For quantification, a dilution series of purified jagaricin in MeOH/water 3:1 was performed, and the individual samples were analysed by the described method. Besides authentic samples, a set of two quality control samples were analysed regularly.

3. Results and discussion

3.1. Medium development based on host composition

Janthinobacterium agaricidamnosum is causing a soft rot disease when getting in contact with its host, e.g. the cultured mushroom *Agaricus bisporus*. The mushroom fruiting bodies get lysed within hours (Graupner et al., 2012) via the pore-forming activity of jagaricin (Fischer et al., 2019). Through the lysis of the mushrooms' fruiting body, all nutrients become available to *J. agaricidamnosum*. The cell wall of *A. bisporus* fruiting bodies is a rich source of polysaccharides like mannans (monomer: mannose) and β-D-glucans (monomer: glucose) (Novaes-Ledieu and Mendoza, 1981; Sharma et al., 2014). Furthermore, fructose and the sugar alcohol mannitol are also present in the cytoplasm, where mannitol is synthesized via fructose and used as storage carbon (Meena et al., 2015; Patel and Williamson, 2016).

Based on this information, different carbon sources were chosen to modify the standard complex medium used by Fischer et al. (2019), which contained glucose as dominant the carbon source. In addition, glycerol as well as $CaCO_3$, the latter was originally used as pH buffer, were left out in this study. The results of the microtiter plate screening of media compositions are depicted in Fig. 1. Glucose as a reference, fructose, mannose, mannitol and sucrose were chosen. The disaccharide sucrose is known as a slow release carbon source consisting of the monomers glucose and fructose (Reid and Abratt, 2005; Wang et al., 2004). Thus, it was assumed that the final jagaricin concentration should be higher than the reference but lower than with pure fructose. Furthermore, sucrose is often used as a low-cost carbon source with the additional benefit of lower osmotic pressure in comparison to an equal amount of glucose monomers, which is an important aspect in osmotic sensitive plant cell fermentation (Haswell and Verslues, 2015; Sumaryono et al., 2012). Fig. 1A shows the scattered light signal of all cultivations, reflecting biomass formation. In general, all carbon sources are suitable to generate biomass, with the propensity increasing from mannose (smallest slope/growth rate) to sucrose (highest slope/growth rate). The stationary phase is reached between 24 and 40 h, depending on the carbon source. Since it was unknown, whether jagaricin formation is growth-related, the experiment was finished after a longer stationary phase at 60 h. In Fig. 1B significant differences in final jagaricin concentrations for the experiments became obvious. For all carbon sources, jagaricin could be detected. Only 16.3 mg L^{-1} were formed in the reference cultivation with glucose. The usage of mannose results in a similar final jagaricin concentration of 17.9 mg L^{-1}. Mannose is a C2-epimer of glucose (Sharma et al., 2014) and therefore structurally and chemically similar. The final jagaricin concentration with sucrose

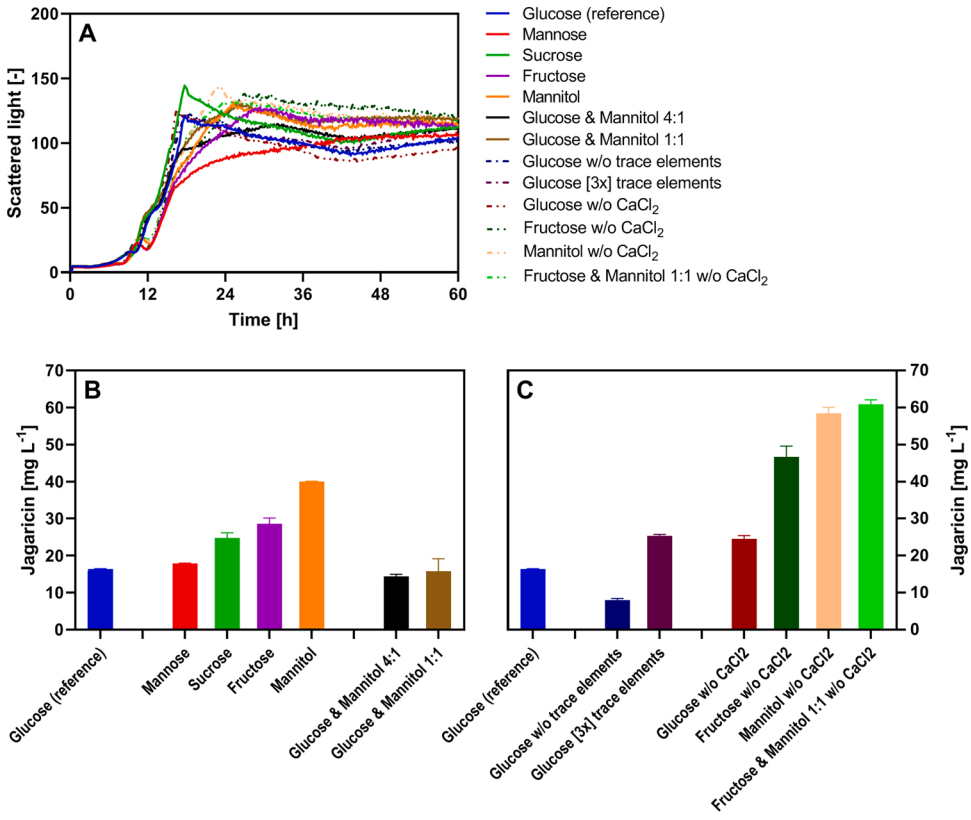

Fig. 1. Impact of carbon sources and $CaCl_2$ on growth of *J. agaricidamnosum* and jagaricin formation. **A:** Growth curves recorded by scattered light for different carbon sources, selected carbon sources with and without $CaCl_2$ and mixtures of carbon sources with and without $CaCl_2$. Total concentration for all carbon sources was 10 g L^{-1} per constellation. **B:** Jagaricin concentrations (N = 2) obtained after 60 h for different carbon sources and ratios against glucose as reference. **C:** Jagaricin concentrations (N = 2) obtained after 60 h by using different concentrations of trace element solution as well as decreasing the amount of calcium chloride against glucose as reference. Experimental conditions: BioLector® system, temperature = 25 °C; shaking frequency =1000 rpm; filling volume =1 mL; initial pH = 6.50 (buffered with 50 mM MOPS); 0.5 g L^{-1} $CaCl_2 \times 2\ H_2O$.

(24.7 mg L^{-1}) is, as expected, between the pure glucose and pure fructose (28.6 mg L^{-1}). The cultivation based on mannitol resulted in a final concentration of 40 mg L^{-1} of jagaricin, which is a significant increase by 145 % over the glucose-based reference. This result supports the chosen strategy to mimic the composition of the mushroom fruiting bodies. From a physicochemical point of view, it is yet difficult to give a satisfying explanation for the positive effect of mannitol on the jagaricin formation. In comparison to the sugars, mannitol is a reduced agent and works as an osmoprotectant (Meena et al., 2015; Patel and Williamson, 2016). The osmotic pressure in the meaning of osmotic stress is a well-known trigger for some secondary metabolites (Pan et al., 2019) and could therefore influence the jagaricin formation. As shown in the experimental results of the Supplementary Fig. S1, osmotic pressure can be excluded as a trigger, and high values even lower the jagaricin formation. To clarify if mannitol serves not only as a carbon source but also as a trigger substance for jagaricin formation, two mixtures of mannitol and glucose were tested. Surprisingly, none of the mixtures resulted in higher concentrations of jagaricin compared to glucose alone (Fig. 1B).

A. bisporus fruiting bodies are a rich source of trace elements like iron (Reis et al., 2012; Sesli et al., 2008) which is already mirrored by the used trace element solution. The most dominant component is iron (III) citrate. Iron is a key parameter in transcriptional control of microbial secondary metabolism in general (Weinberg, 1969, 1990) and well-known to increase lipopeptide production (Cooper et al., 1981; Wei et al., 2004). To elucidate the relevance and impact of this trace element solution on jagaricin formation, cultivations were performed without any trace element solution as well as with a three-fold amount. The scattered light measurements in Fig. 1A show that neither absence nor triplication of the trace element solution has an impact on biomass formation. However, a clear impact is visible with respect to the final jagaricin concentration. Without addition of trace elements, the jagaricin concentration decreased to 8 mg L^{-1}. On the contrary, the three-fold amount increased the jagaricin concentration by 53 % to 25 mg L^{-1} (Fig. 1C).

Based on the assumption that mushroom fruiting bodies do not contain relevant amounts of calcium, the omission from the original medium was investigated. Originally, calcium chloride was added to prevent lipopeptide monolayers and thus reduce foaming (Yang and Yang, 2010). As depicted in Fig. 1C, the removal of $CaCl_2$ resulted in a strong increase of jagaricin concentration for the three carbon sources glucose, fructose, and mannitol. The combination of mannitol without $CaCl_2$ increased the final jagaricin concentration by 258 % compared to the reference (Fig. 1C).

Underlying the metabolic pathways from the Kyoto Encyclopedia of Genes and Genomes (Kanehisa and Goto, 2000), mannitol could be converted into fructose via mannitol 2-dehydrogenase [enzyme commission number EC 1.1.1.67]. Thus, to evaluate additive effects like bottlenecks for both carbon sources, a mixture of 1:1 (w/w) mannitol and fructose were tested. Based on the previous results, a final jagaricin concentration of at least 52.5 mg L^{-1} was expected. With a value of 60.9 mg L^{-1}, the measured concentration was 16 % higher and is in line with the results obtained with pure mannitol without $CaCl_2$. Thus, in combination with fructose, mannitol seems to play a more important role in enhancing product formation. For this reason and since the final jagaricin concentration of 60.9 mg L^{-1} (an increase of 274 % compared to the glucose reference) was the highest measured value so far, it was decided to continue with this setup for subsequent experiments. Additionally, from an economic point of view, fructose is a less costly substrate than mannitol, improving the cost-of-goods ratio for further scale-up experiments.

3.2. Impact of oxygen availability

It has been reported for several cases of lipopeptide production that oxygen supply can be a critical parameter to influence the product formation (Fahim et al., 2012; Ghribi and Ellouze-Chaabouni, 2011). To investigate the impact of oxygen supply on the jagaricin formation, shake flask experiments were conducted using the TOM device®, which

enables the online measurement of the oxygen uptake as well as the carbon dioxide formation (Fig. 2). Through variation of the filling volume in the shake flasks (10 | 15 | 20 | 30 mL), different maximum oxygen transfer rates (OTR_{max}) and therefore different levels of oxygen supply could be obtained (Meier et al., 2016). To focus the experiment on the elucidation of oxygen supply on jagaricin formation and to eliminate the effect of different biomass concentrations, a common strategy is to separate the experiment into two different phases (Heyman et al., 2019). The first phase was conducted under oxygen-unlimited conditions at a high shaking frequency of 300 rpm to generate equal biomass concentrations in all experimental setups. As depicted in Fig. 2A, all OTR curves are nearly identical and show a very similar metabolic activity as expected. The second phase was initiated after reaching an OTR-value of 26 mmol L^{-1} h^{-1}. Besides the reference cultivation, the shaking frequency was reduced in all experiments to a significantly lower value of 125 rpm to enforce different levels of oxygen limitation in dependency of the filling volume. After switching the shaking frequency, all cultures were oxygen-limited as indicated by typical plateaus of the OTR (Anderlei and Büchs, 2001). The lowest filling volume of 10 mL reaches the highest OTR with approximately 21 mmol L^{-1} h^{-1} and in contrast the highest filling volume of 30 mL results in the lowest OTR of 9 mmol L^{-1} h^{-1}. For the filling volumes of 10 and 15 mL, a drastic drop in the OTR curve was noted after 16 and 19.5 h, respectively. This drop correlates with the consumption of mannitol, as validated by the offline measured samples (Fig. 2B). For the higher filling volumes of 20 and 30 mL, this drop was not obvious since it is covered by the effect of the oxygen limitation. The final drop in all OTR curves indicates the depletion of fructose, also validated by the offline measurements depicted in Fig. 2B. The oxygen unlimited reference, which was shaken continuously at 300 rpm, reached a maximum OTR of 34 mmol L^{-1} h^{-1}. Mannitol was fully consumed after 17.7 h and fructose after 26 h, as shown in the offline data in Fig. 1B.

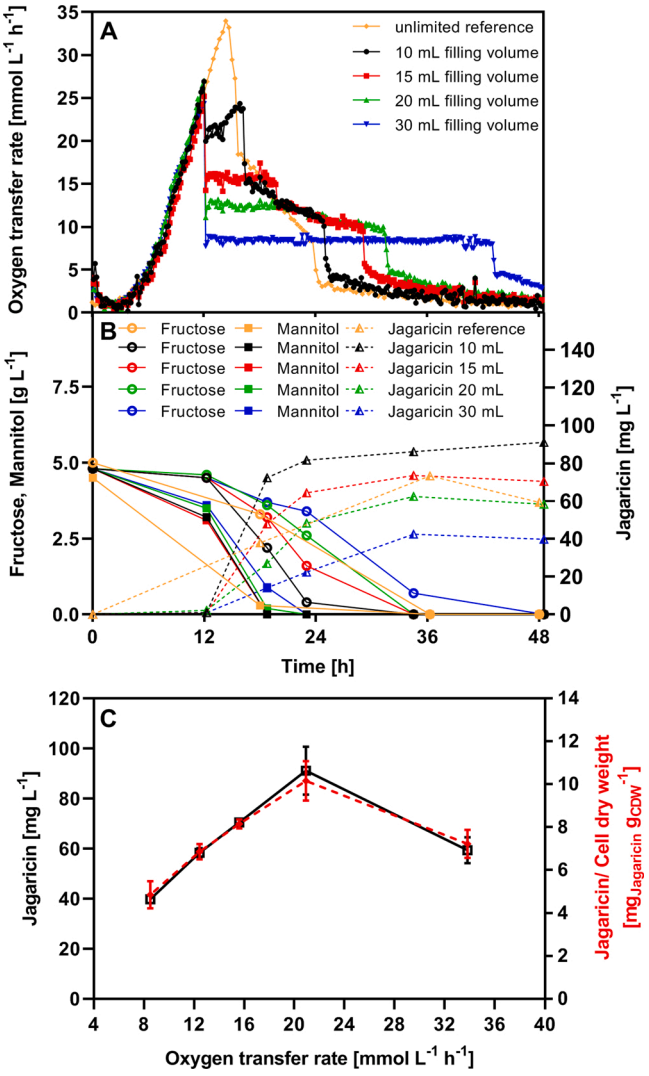

Fig. 2. Impact of oxygen availability on jagaricin formation. **A:** Oxygen transfer rates (OTR) for four different filling volumes. After an initial unlimited growth phase till the 12.25 h the shaking frequency was reduced from 300 to 125 rpm for limited growth conditions. **B:** Depletion of fructose and mannitol and the formation of jagaricin are shown. **C:** Jagaricin and cell dry weight specific jagaricin of the final samples after 48.5 h plotted over the maximum OTR reached in each filling volume. Cultivation conditions: 250 mL shake flasks; temperature 25 °C; filling volumes 10 | 15 | 20 | 30 mL; shaking frequencies were 300 and 125 rpm; shaking diameter 50 mm, initial pH = 6.50 (buffered with 100 mM MOPS).

With respect to jagaricin formation, a clear trend becomes obvious in Fig. 2B. With decreasing filling volume, respectively increasing OTR, the jagaricin concentration increased from 40 mg L^{-1} to 91 mg L^{-1}. However, Fig. 2B and C show that there is an optimal working point and a short period of oxygen limitation seems to trigger a stronger formation of jagaricin in comparison to the oxygen-unlimited reference experiment. This cannot be attributed to different biomass concentrations, since these were very similar in all shake flasks. As illustrated in Fig. 2C, the cell dry weight (CDW)-specific jagaricin value was calculated and plotted for the final jagaricin concentration. An impact of oxygen supply on a lipopeptide formation was also investigated for surfactin and fengycin by Fahim et al. (2012).

3.3. Scale-up and jagaricin trigger

To generate larger amounts of jagaricin for further functional investigations and to receive more detailed sampling kinetics, the shake flask conditions were scaled up into 7 L stirred tank bioreactor. To separate the effects of scale-up from any influence caused by an active pH-control, the experiment was conducted with pH-buffer similar to the conditions in shake flask experiments. To limit the maximum OTR to the optimal value of 21 mmol h L^{-1}, the stirring rate was adjusted to a maximum value of 777 rpm and the aeration rate was fixed at 0.5 vvm.

As seen in Fig. 3A the overlay of the scaled-up OTR curve and the shake flask reference (TOM reference) perfectly match, thus indicating a successful scale-up. Furthermore, the preferable consumption of mannitol over fructose is confirmed through a tight sampling schedule. Mannitol is consumed shortly after 16.5 h, indicated by a fast drop of the OTR (dotted line #3). Whereas fructose is depleted between 21.5 and 36 h, presumably, shortly after 24 h (fast drop in OTR at dotted line #4). As seen in the offline data in Fig. 3B, mannose was formed during the consumption of mannitol, reaching a stable maximum at 100 mg L^{-1} before it was reutilized after the depletion of mannitol and ongoing consumption of fructose. A reaction pathway from the Kyoto Encyclopedia of Genes and Genomes KEGG (Kanehisa and Goto, 2000) and *J. agaricidamnosum* genomic analysis (Graupner et al., 2015) suggests that mannose could be biosynthesized from mannitol through fructose. The active enzymes hereby are mannitol 2-dehydrogenase [enzyme commission number, EC 1.1.1.67], fructokinase [EC 2.7.1.4], mannose-6-phosphate isomerase [EC 5.3.1.8], and a mannose PTS system EIIA component [EC 2.7.1.191]. Mannose could thus be a storage intermediate since mannitol utilization could have a bottleneck.

The pH increased from an initial of 6.50 to up to 7.69 after 60 h of fermentation time (Fig. 3A). Notably, the pH shows two minor drops at the depletion events of the carbon sources (#3 and #4), presumably correlating with metabolic switching. However, the pH also shows a slight decrease within those two depletion events. Latter could indicate the formation of acidic intermediates. Surprisingly, the OTR indicates a second substrate limitation, starting after the consumption of glutamic acid (dotted line #2) and lasting till the depletion of fructose (dotted line

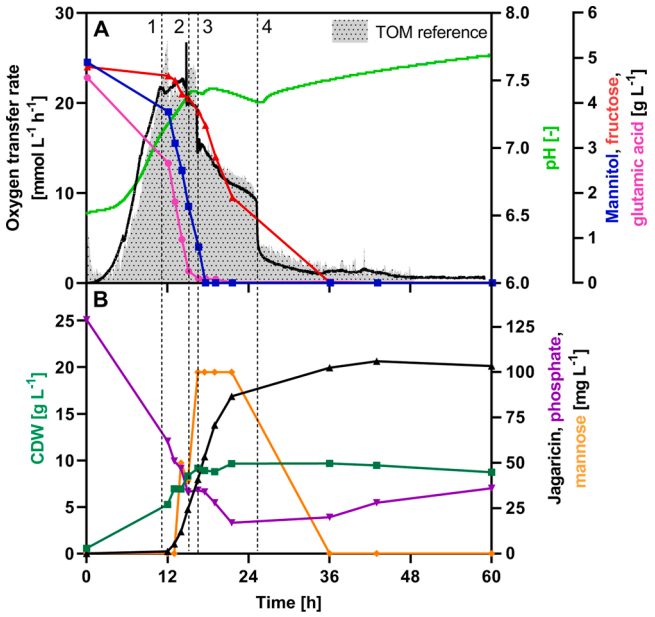

Fig. 3. Batch fermentation of *J. agaricidamnosum* DSM 9628 with optimized medium. Scale-up of shake-flask conditions to a 7-L stirred tank bioreactor. **A:** Process parameters oxygen transfer rate (OTR) and pH as well as offline analytics of carbon sources (mannitol, fructose) and glutamic acid. The stirring rate was adjusted to 777 rpm to obtain an OTR of 21 mmol L^{-1} h^{-1}. **B:** Phosphate and product analytics (jagaricin, mannose) as well as the biomass, calculated as cell dry weight (CDW). The dotted vertical lines mark different events. A maximum jagaricin concentration reached was 106 mg L^{-1}. Fermentation conditions: Filling volume = 4 L; temperature = 25 °C; aeration rate = 0.5 vvm; pH was initially adjusted to 6.50 ± 0.05 with NaOH and buffered with 100 mM MOPS.

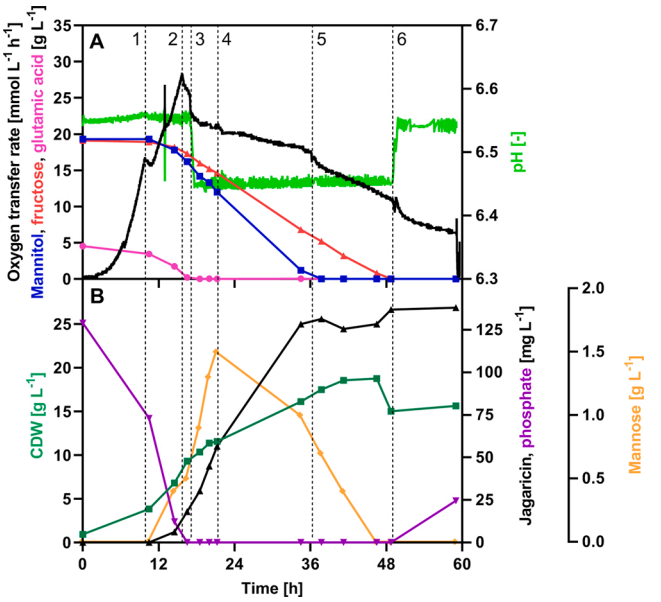

Fig. 4. Batch fermentation of *J. agaricidamnosum* DSM 9628 with optimized medium in 7-L stirred tank bioreactor. **A:** Process parameters oxygen transfer rate (OTR) and pH as well as offline analytics of carbon sources (mannitol, fructose) and glutamic acid. **B:** Phosphate and product analytics (jagaricin, mannose) as well as the biomass, calculated as cell dry weight (CDW). The dotted vertical lines mark different events. A maximum jagaricin concentration reached was 138 mg L^{-1}. Fermentation conditions: Filling volume = 4 L; temperature = 25 °C; DOT ≥ 20 %; aeration rate = 0.5 vvm; pH 6.50 ± 0.05 (with 10 % H_2SO_4 and 12.5 % NH_4OH).

#4). This limitation could be responsible for the stagnation of the cell dry weight. As obvious from Fig. 3B, the biomass reached a stable concentration shortly before the depletion of mannitol, with a maximum CDW of 9.67 g L^{-1} at 36 h.

The formation of jagaricin started at about 12 h, visible in a minor drop of the OTR curve (dotted line #1), and reached a maximum of 106 mg L^{-1} after 43 h. Compared to the CDW-specific jagaricin concentration in the shake flask experiment (10.2 $mg_{Jagaricin} \cdot g_{CDW}^{-1}$), the scale-up successfully achieved a CDW-specific jagaricin concentration of 10.6 $mg_{Jagaricin} \cdot g_{CDW}^{-1}$ after 36 h.

To investigate the impact of higher amounts of carbon sources the initial concentrations of mannitol and fructose were increased four-fold in subsequent experiments to 20 g L^{-1} each. This made an active pH control essential, which was implemented with 10 % H_2SO_4 and 12.5 % NH_4OH as titration media. An additional aspect, besides scale-up, was to investigate the impact of a phosphate limitation on the overall process, although the mushroom is, in general a very rich source of phosphate (Muszyńska et al., 2017). Nevertheless, phosphate limitation is a very common way to provoke the formation of secondary metabolites and was therefore included in our evaluation.

Also here, the metabolic activity during cultivation can be observed online by following the OTR signal. As depicted in Fig. 4A, the OTR increased exponentially until 6.5 h. At this time point, diauxic behavior was obvious, indicated by a step in the OTR curve, which can be attributed to the depletion of amino acids from the supplied yeast extract and the beginning of mannitol and fructose consumption. The OTR further increased to a maximum value of 28 mmol L^{-1} h^{-1} at 15.7 h. The following decrease of the OTR is caused by a second substrate limitation, which can be attributed to phosphate depletion at 15.7 h. Since jagaricin formation is triggered in a time window between 9.5 and 15.7 h (dotted line #1 in Fig. 4B), phosphate depletion (entered after 15.8 h; dotted line #2) can be excluded as a classical trigger. Nevertheless, it is very likely that another nutrient limitation is the potential trigger for jagaricin formation. Therefore, all amino acids were analysed in detail. The most dominating amino acid provided is glutamic acid, which is completely taken up after 16.9 h, indicated by a fast switch in pH (dotted line #3). Since jagaricin formation starts before depletion of glutamic acid, its limitation can also be excluded as a trigger.

Besides the trigger for jagaricin formation, the overall trend and final concentration are also of high importance. In comparison to the scale-up fermentation, an increase of jagaricin concentration can be seen until 37.8 h, which correlates with the depletion of mannitol at 36 h, indicated by a small drop in the OTR curve (dotted line #5). Although, both carbon sources were consumed simultaneously (already seen in Fig. 3), it became obvious that mannitol could be of higher importance for the jagaricin formation. Therefore, mannitol metabolism was analysed more deeply. The consumption of mannitol by *J. agaricidamnosum* leads to the formation of the intermediate monomer mannose. As shown in Fig. 4B, an increasing concentration of mannose could be detected in the supernatant between 10.5–21.25 h (dotted line #4). The maximum value of mannose remains unknown since no offline samples between 21.25 and 34.5 h were taken. In the biochemical pathways described above, the mannitol 2-dehydrogenase catalyzes the reaction from mannitol to fructose by using NAD + as an acceptor. This leads to an additional NAD + regeneration (Blank et al., 2010) compared to the other sugars tested, which could positively impact the NADH-exhaustive fatty acid biosynthesis. Since jagaricin biosynthesis is based on 3(R)-hydroxy myristic acid as the fatty acid moiety precursor, the utilization of mannitol could therefore indirectly support jagaricin synthesis (Cronan and Thomas, 2009). Supporting this hypothesis, jagaricin synthesis almost completely terminated with the exhaustion of mannitol at 36 h, while both the intermediate mannose and the co-substrate fructose were still available. Thus, only the initial oxidation processes of mannitol correlate clearly with jagaricin synthesis.

Biomass formation, however, seems to be essential for jagaricin

production. The offline samples for CDW are presented in Fig. 4B. Interestingly, it was assumed that CDW formation will be limited by the depletion of phosphate at 16.5 h. However, after a short drop, CDW concentration continued to increase up to 18.75 g L^{-1} until the depletion of fructose, which clearly indicates that additional organic phosphate was released by the complex compounds. Overall, the fermentation resulted in a maximum concentration of 138 mg L^{-1} jagaricin at 59 h, which is about 3.1-fold higher compared to the standard glucose medium (see Supplementary Fig. S2). In comparison to the scale-up experiment in Fig. 3, the CDW-specific jagaricin concentration declined by 25 % to 8 $mg_{Jagaricin} \cdot g_{CDW}^{-1}$ although the carbon source was four-fold. Since phosphate limitation is no key parameter to trigger and increase the formation of jagaricin, in contrast to many other secondary metabolites producing processes, additional cultivation was performed with higher availability of free phosphate.

To ensure unlimited conditions, phosphoric acid was used for pH control in the cultivation presented in Fig. 5. Due to the uptake of amino acids until 16.4 h, phosphoric acid was added to the medium and increased the phosphate concentration up to 840 mg L^{-1} (Fig. 5B, dotted line #2). The unlimited access to phosphate is reflected by higher OTR values in general and therefore a higher metabolic activity in comparison to the previous cultivations. Consequently, both carbon sources were already depleted after 32.2 h (dotted lines #3 and #4), which is significantly faster in comparison to the previous cultivation ending after 48.8 h.

Most remarkable is the trend of the jagaricin concentration, which reached its maximum value of 251 mg L^{-1} at 43.5 h. This is an increase of approximately 458 % in comparison to previous results in the standard glucose medium (see Supplementary, Fig. S2). Also, the CDW-specific jagaricin concentration increased to 15.5 $mg_{Jagaricin} \cdot g_{CDW}^{-1}$ at 40 h. The CDW-specific jagaricin concentration, thus, almost doubled compared to the former experiment and is the so far highest concentration observed in this study. Possible explanations for the beneficial impact of phosphate on the jagaricin formation can be given considering the metabolic pathways in the Kyoto Encyclopedia of Genes and Genomes KEGG (Kanehisa and Goto, 2000) combined with the known *J. agaricidamnosum* genomics data (Graupner et al., 2015).

Fructose, respectively mannitol, can be taken up by ATP binding cassette transporter systems, so-called ABC-transporters (Lambert et al., 2001; Schneider, 2001). These transporters need energy (ATP). As discussed above, the fermentation with phosphate showed higher metabolic activity, since the maximum OTR value of 45 mmol L^{-1} h^{-1} was 61 % higher compared to the previous fermentation (28 mmol L^{-1} h^{-1}). The maximum CDW instead decreased by 19 % to a maximum of 15.28 g L^{-1} after 40 h. This higher oxygen demand on the one hand, and less biomass on the other, could indicate a higher ATP generation. For the accelerated uptake of mannitol and fructose and finally for the overall production of jagaricin via the non-ribosomal peptide synthetases, the higher ATP generation would be beneficial (Schwarzer et al., 2003; Schwarzer and Marahiel, 2001).

4. Conclusion

In this study, a biotechnological process for the formation of the antifungal cyclic lipopeptide jagaricin was developed. It was demonstrated that a medium composition based on the composition of the fungal host *A. bisporus* enables a significant increase of the final jagaricin concentration. It was shown that a short time frame of oxygen limitation supports the formation of jagaricin. Moreover, it became clear that a classic phosphate limitation does not trigger or support the formation of jagaricin. In contrast, a high availability of phosphate seems to be important for an enhanced formation of jagaricin. Ultimately, a final maximum jagaricin concentration of 251 mg L^{-1} could be achieved, which is an increase of 458 % in comparison to previous results in the standard glucose medium (see Supplementary, Fig. S2). Although further optimizations are possible and a definite trigger for inducing jagaricin synthesis could not be resolved in this work, this concentration allows the production of sufficient amounts of jagaricin to enable further experiments towards the elucidation of the bioactive potential of this substance.

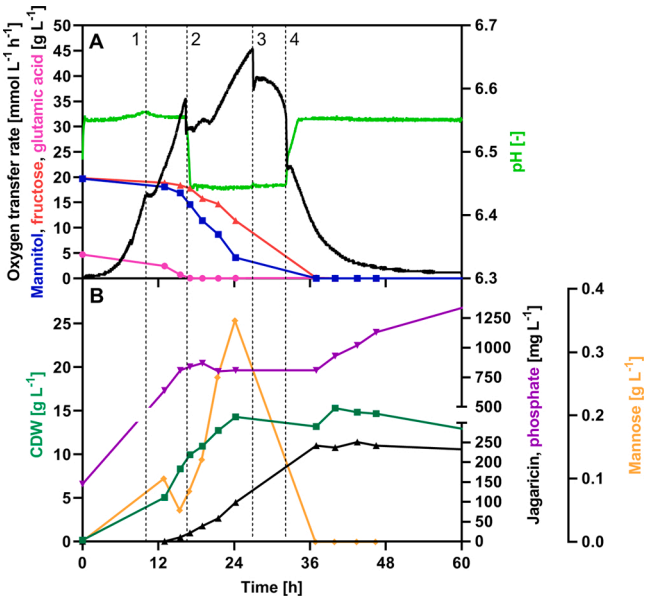

Fig. 5. Batch fermentation of *J. agaricidamnosum* DSM 9628 with optimized medium in a 7-L stirred tank bioreactor and phosphoric acid as pH regulator. **A:** Process parameters oxygen transfer rate (OTR) and pH as well as the offline analytics of the carbon sources (mannitol, fructose) and glutamic acid. **B:** Phosphate and offline product analytics (jagaricin, mannose) as well as the biomass, calculated as cell dry weight (CDW). A maximum jagaricin concentration of 251 mg L^{-1} was reached. The dotted vertical lines mark different events. Fermentation conditions: Filling volume = 4 L; temperature = 25 °C; DOT ≥ 20 %; aeration rate = 0.5 vvm; pH = 6.50 ± 0.05 (with 10 % H_3PO_4 and 12.5 % NH_4OH).

CRediT authorship contribution statement

Nicolas Schlosser, **Miriam A. Rosenbaum** and **Lars Regestein** have written the manuscript. **Nicolas Schlosser** and **Jordi Espino-Martínez** conducted all cultivations. **Florian Kloss**, **Florian Meyer**, **Bettina Bardl** developed and performed all analytical methods. **Lars Regestein** supervised the study.

Declaration of Competing Interest

All authors agree on the final version of the manuscript. The authors have declared no conflict of interest.

Acknowledgements

L.R., N.S. and B.B. are supported by the Free State of Thuringia (project number 2019 FGR 0079). N.S. was supported by the International Leibniz Research School for Microbial and Biomolecular Interactions (ILRS). F.K. and F.M were supported by Infect Control (03ZZ0835A and 03ZZ0826A). The authors thank Gudrun Krauter and Michael Cyrulies for their helpful technical support during fermentations and analytics.

Appendix A. Supplementary data

Supplementary material related to this article can be found, in the online version, at doi:https://doi.org/10.1016/j.jbiotec.2021.06.015.

References

Anderlei, T., Büchs, J., 2001. Device for sterile online measurement of the oxygen transfer rate in shaking flasks. Biochem. Eng. J. 7 (2), 157–162. https://doi.org/10.1016/S1369-703X(00)00116-9.

Anderlei, T., Zang, W., Papaspyrou, M., Büchs, J., 2004. Online respiration activity measurement (OTR, CTR, RQ) in shake flasks. Biochem. Eng. J. 17 (3), 187–194. https://doi.org/10.1016/s1369-703x(03)00181-5.

Biniarz, P., Lukaszewicz, M., 2017. Direct quantification of lipopeptide biosurfactants in biological samples via HPLC and UPLC-MS requires sample modification with an organic solvent. Appl. Microbiol. Biotechnol. 101 (11), 4747–4759. https://doi.org/10.1007/s00253-017-8272-y.

Blank, L.M., Ebert, B.E., Buehler, K., Bühler, B., 2010. Redox biocatalysis and metabolism: molecular mechanisms and metabolic network analysis. Antioxid. Redox Signal. 13 (3), 349–394. https://doi.org/10.1089/ars.2009.2931.

Blesken, C.C., Strumpfler, T., Tiso, T., Blank, L.M., 2020. Uncoupling foam fractionation and foam adsorption for enhanced biosurfactant synthesis and recovery. Microorganisms 8 (12). https://doi.org/10.3390/microorganisms8122029.

Büchs, J., 2001. Introduction to advantages and problems of shaken cultures. Biochem. Eng. J. 7 (2), 91–98.

CDC, 2019. Antibiotic Resistance Threats in the United States, 2019. Retrieved from Atlanta, GA: https://www.cdc.gov/drugresistance/Biggest-Threats.html.

Chauhan, V., Kanwar, S.S., 2020. Lipopeptide(s) associated with human microbiome as potent cancer drug. Semin. Cancer Biol. https://doi.org/10.1016/j.semcancer.2020.06.012.

Chen, W.-C., Juang, R.-S., Wei, Y.-H., 2015. Applications of a lipopeptide biosurfactant, surfactin, produced by microorganisms. Biochem. Eng. J. 103, 158–169. https://doi.org/10.1016/j.bej.2015.07.009.

Cooper, D.G., Macdonald, C.R., Duff, S.J., Kosaric, N., 1981. Enhanced production of surfactin from *Bacillus subtilis* by continuous product removal and metal cation additions. Appl. Environ. Microbiol. 42 (3), 408–412.

Coutte, F., Lecouturier, D., Dimitrov, K., Guez, J.S., Delvigne, F., Dhulster, P., Jacques, P., 2017. Microbial lipopeptide production and purification bioprocesses, current progress and future challenges. Biotechnol. J. 12 (7) https://doi.org/10.1002/biot.201600566.

Cronan, J.E., Thomas, J., 2009. Bacterial fatty acid synthesis and its relationships with polyketide synthetic pathways. Meth. Enzymol. 459, 395–433. https://doi.org/10.1016/S0076-6879(09)04617-5.

Cross, S.A., Scott, L.J., 2008. Micafungin: a review of its use in adults for the treatment of invasive and oesophageal candidiasis, and as prophylaxis against Candida infections. Drugs 68 (15), 2225–2255. https://doi.org/10.2165/00003495-200868150-00010.

Duarte, C., Gudiña, E.J., Lima, C.F., Rodrigues, L.R., 2014. Effects of biosurfactants on the viability and proliferation of human breast cancer cells. AMB Express 4. https://doi.org/10.1186/s13568-014-0040-0, 40-40.

Fahim, S., Dimitrov, K., Gancel, F., Vauchel, P., Jacques, P., Nikov, I., 2012. Impact of energy supply and oxygen transfer on selective lipopeptide production by *Bacillus subtilis* BBG21. Bioresour. Technol. 126, 1–6. https://doi.org/10.1016/j.biortech.2012.09.019.

Fischer, D., Gessner, G., Fill, T.P., Barnett, R., Tron, K., Dornblut, K., Kloss, F., Stallforth, P., Hube, B., Heinemann, S.H., Hertweck, C., Scherlach, K., Brunke, S., 2019. Disruption of membrane integrity by the bacterium-derived antifungal jagaricin. Antimicrob. Agents Chemother. 63 (9) https://doi.org/10.1128/AAC.00707-19.

Funke, M., Buchenauer, A., Schnakenberg, U., Mokwa, W., Diederichs, S., Mertens, A., Muller, C., Kensy, F., Büchs, J., 2010. Microfluidic biolector-microfluidic bioprocess control in microtiter plates. Biotechnol. Bioeng. 107 (3), 497–505. https://doi.org/10.1002/bit.22825.

Geudens, N., Martins, J.C., 2018. Cyclic lipodepsipeptides from *Pseudomonas* spp. - biological swiss-army knives. Front. Microbiol. 9, 1867. https://doi.org/10.3389/fmicb.2018.01867.

Ghribi, D., Ellouze-Chaabouni, S., 2011. Enhancement of *Bacillus subtilis* lipopeptide biosurfactants production through optimization of medium composition and adequate control of aeration. Biotechnol. Res. Int. 2011, 653654 https://doi.org/10.4061/2011/653654.

Gonzalez-Jaramillo, L.M., Aranda, F.J., Teruel, J.A., Villegas-Escobar, V., Ortiz, A., 2017. Antimycotic activity of fengycin C biosurfactant and its interaction with phosphatidylcholine model membranes. Colloids Surf. B 156, 114–122. https://doi.org/10.1016/j.colsurfb.2017.05.021.

Götze, S., Stallforth, P., 2019. Structure, properties, and biological functions of nonribosomal lipopeptides from pseudomonads. Nat. Prod. Rep. https://doi.org/10.1039/C9NP00022D.

Graupner, K., Scherlach, K., Bretschneider, T., Lackner, G., Roth, M., Gross, H., Hertweck, C., 2012. Imaging mass spectrometry and genome mining reveal highly antifungal virulence factor of mushroom soft rot pathogen. Angew. Chem. Int. Ed. Engl. 51 (52), 13173–13177. https://doi.org/10.1002/anie.201206658.

Graupner, K., Lackner, G., Hertweck, C., 2015. Genome sequence of mushroom soft-rot pathogen *Janthinobacterium agaricidamnosum*. Genome Announc. 3 (2) https://doi.org/10.1128/genomeA.00277-15.

Haack, F.S., Poehlein, A., Kroger, C., Voigt, C.A., Piepenbring, M., Bode, H.B., Daniel, R., Schafer, W., Streit, W.R., 2016. Molecular keys to the Janthinobacterium and Duganella spp. interaction with the plant pathogen Fusarium graminearum. Front. Microbiol. 7, 1668. https://doi.org/10.3389/fmicb.2016.01668.

Hamley, I.W., 2015. Lipopeptides: from self-assembly to bioactivity. Chem. Commun. (Camb.) 51 (41), 8574–8583. https://doi.org/10.1039/c5cc01535a.

Haswell, E.S., Verslues, P.E., 2015. The ongoing search for the molecular basis of plant osmosensing. J. Gen. Physiol. 145 (5), 389–394. https://doi.org/10.1085/jgp.201411295.

Heyman, B., Tulke, H., Putri, S.P., Fukusaki, E., Büchs, J., 2019. Online monitoring of the respiratory quotient reveals metabolic phases during microaerobic 2,3-butanediol production with *Bacillus licheniformis*. Eng. Life Sci. 20 (3–4), 133–144. https://doi.org/10.1002/elsc.201900121.

Ines, M., Dhouha, G., 2015. Lipopeptide surfactants: production, recovery and pore forming capacity. Peptides 71, 100–112. https://doi.org/10.1016/j.peptides.2015.07.006.

Kanehisa, M., Goto, S., 2000. KEGG: kyoto encyclopedia of genes and genomes. Nucleic Acids Res. 28 (1), 27–30. https://doi.org/10.1093/nar/28.1.27.

Kornberger, A., Luchting, B., Kur, F., Weis, M., Weis, F., Stock, U.A., Beiras-Fernandez, A., 2016. Daptomycin for the treatment of major gram-positive infections after cardiac surgery. J. Cardiothorac. Surg. 11 (1), 120. https://doi.org/10.1186/s13019-016-0519-7.

Lambert, A., Østeråas, M., Mandon, K., Poggi, M.-C., Le Rudulier, D., 2001. Fructose uptake in *Sinorhizobium meliloti* is mediated by a high-affinity ATP-binding cassette transport system. J. Bacteriol. 183 (16), 4709–4717. https://doi.org/10.1128/jb.183.16.4709-4717.2001.

Lattermann, C., Funke, M., Hansen, S., Diederichs, S., Büchs, J., 2014. Cross-section perimeter is a suitable parameter to describe the effects of different baffle geometries in shaken microtiter plates. J. Biol. Eng. 8, 18. https://doi.org/10.1186/1754-1611-8-18.

Lincoln, S.P., Fermor, T.R., Tindall, B.J., 1999. *Janthinobacterium agaricidamnosum* sp. nov., a soft rot pathogen of *Agaricus bisporus*. Int. J. Syst. Bacteriol. 49 (Pt 4), 1577–1589. https://doi.org/10.1099/00207713-49-4-1577.

Martin, J.F., 2004. Phosphate control of the biosynthesis of antibiotics and other secondary metabolites is mediated by the PhoR-PhoP system: an unfinished story. J. Bacteriol. 186 (16), 5197–5201. https://doi.org/10.1128/JB.186.16.5197-5201.2004.

Meena, K.R., Kanwar, S.S., 2015. Lipopeptides as the antifungal and antibacterial agents: applications in food safety and therapeutics. Biomed. Res. Int. 2015, 473050 https://doi.org/10.1155/2015/473050.

Meena, M., Prasad, V., Zehra, A., Gupta, V.K., Upadhyay, R.S., 2015. Mannitol metabolism during pathogenic fungal-host interactions under stressed conditions. Front. Microbiol. 6 https://doi.org/10.3389/fmicb.2015.01019, 1019-1019.

Meier, K., Klöckner, W., Bonhage, B., Antonov, E., Regestein, L., Büchs, J., 2016. Correlation for the maximum oxygen transfer capacity in shake flasks for a wide range of operating conditions and for different culture media. Biochem. Eng. J. 109, 228–235. https://doi.org/10.1016/j.bej.2016.01.014.

Mnif, I., Ghribi, D., 2015. Review lipopeptides biosurfactants: mean classes and new insights for industrial, biomedical, and environmental applications. Biopolymers 104 (3), 129–147. https://doi.org/10.1002/bip.22630.

Morrison, V.A., 2005. Caspofungin: an overview. Expert Rev. Anti Ther. 3 (5), 697–705. https://doi.org/10.1586/14787210.3.5.697.

Muszyńska, B., Kała, K., Rojowski, J., Grzywacz, A., Opoka, W., 2017. Composition and biological properties of *Agaricus bisporus* fruiting bodies – a review. Polish J. Food Nutr. Sci. 67 (3), 173–181. https://doi.org/10.1515/pjfns-2016-0032.

Novaes-Ledieu, M., Mendoza, C.G., 1981. The cell walls of *Agaricus bisporus* and *Agaricus campestris* fruiting body hyphae. Can. J. Microbiol. 27 (8), 779–787. https://doi.org/10.1139/m81-121.

Pan, R., Bai, X., Chen, J., Zhang, H., Wang, H., 2019. Exploring structural diversity of microbe secondary metabolites using OSMAC strategy: a literature review. Front. Microbiol. 10 (294) https://doi.org/10.3389/fmicb.2019.00294.

Patel, T.K., Williamson, J.D., 2016. Mannitol in plants, fungi, and plant-fungal interactions. Trends Plant Sci. 21 (6), 486–497. https://doi.org/10.1016/j.tplants.2016.01.006.

Pudełko, K., 2013. The occurrence of soft rot (*Janthinobacterium agaricidamnosum*) in mushroom (*Agaricus bisporus*) crops. J. Plant Prot. Res. 53 (2), 148–153. https://doi.org/10.2478/jppr-2013-0022.

Raaijmakers, J.M., De Bruijn, I., Nybroe, O., Ongena, M., 2010. Natural functions of lipopeptides from *Bacillus* and *Pseudomonas*: more than surfactants and antibiotics. FEMS Microbiol. Rev. 34 (6), 1037–1062. https://doi.org/10.1111/j.1574-6976.2010.00221.x.

Rangarajan, V., Clarke, K.G., 2015. Process development and intensification for enhanced production of *Bacillus* lipopeptides. Biotechnol. Genet. Eng. Rev. 31 (1–2), 46–68. https://doi.org/10.1080/02648725.2016.1166335.

Reid, S.J., Abratt, V.R., 2005. Sucrose utilisation in bacteria: genetic organisation and regulation. Appl. Microbiol. Biotechnol. 67 (3), 312–321. https://doi.org/10.1007/s00253-004-1885-y.

Reis, F.S., Barros, L., Martins, A., Ferreira, I.C., 2012. Chemical composition and nutritional value of the most widely appreciated cultivated mushrooms: an inter-species comparative study. Food Chem. Toxicol. 50 (2), 191–197. https://doi.org/10.1016/j.fct.2011.10.056.

Schneider, E., 2001. ABC transporters catalyzing carbohydrate uptake. Res. Microbiol. 152 (3), 303–310. https://doi.org/10.1016/S0923-2508(01)01201-3.

Schwarzer, D., Marahiel, M.A., 2001. Multimodular biocatalysts for natural product assembly. Naturwissenschaften 88 (3), 93–101. https://doi.org/10.1007/s001140100211.

Schwarzer, D., Finking, R., Marahiel, M.A., 2003. Nonribosomal peptides: from genes to products. Nat. Prod. Rep. 20 (3) https://doi.org/10.1039/b111145k.

Sen, R., Swaminathan, T., 1997. Application of response-surface methodology to evaluate the optimum environmental conditions for the enhanced production of surfactin. Appl. Microbiol. Biotechnol. 47 (4), 358–363. https://doi.org/10.1007/s002530050940.

Sesli, E., Tuzen, M., Soylak, M., 2008. Evaluation of trace metal contents of some wild edible mushrooms from Black sea region, Turkey. J. Hazard. Mater. 160 (2–3), 462–467. https://doi.org/10.1016/j.jhazmat.2008.03.020.

Shaligram, N.S., Singhal, R.S., 2010. Surfactin–a Review on Biosynthesis, Fermentation, Purification and Applications, Vol. 48.

Sharma, V., Ichikawa, M., Freeze, H.H., 2014. Mannose metabolism: more than meets the eye. Biochem. Biophys. Res. Commun. 453 (2), 220–228. https://doi.org/10.1016/j.bbrc.2014.06.021.

Singh, V., Haque, S., Niwas, R., Srivastava, A., Pasupuleti, M., Tripathi, C.K., 2016. Strategies for fermentation medium optimization: an in-depth review. Front. Microbiol. 7, 2087. https://doi.org/10.3389/fmicb.2016.02087.

Sumaryono, Muslihatin, W., Ratnadewi, D., 2012. Effect of carbohydrate source on growth and performance of in vitro sago palm (*Metroxylon sagu* Rottb.) plantlets. Hayati 19 (2), 88–92. https://doi.org/10.4308/hjb.19.2.88.

Taylor, S.D., Palmer, M., 2016. The action mechanism of daptomycin. Bioorg. Med. Chem. 24 (24), 6253–6268. https://doi.org/10.1016/j.bmc.2016.05.052.

Wang, D., Xu, Y., Hu, J., Zhao, G., 2004. Fermentation kinetics of different sugars by apple wine yeast *Saccharomyces cerevisiae*. J. Inst. Brew. 110 (4), 340–346. https://doi.org/10.1002/j.2050-0416.2004.tb00630.x.

Wang, X., Hu, W., Zhu, L., Yang, Q., 2017. *Bacillus subtilis* and surfactin inhibit the transmissible gastroenteritis virus from entering the intestinal epithelial cells. Biosci. Rep. 37 (2), BSR20170082 https://doi.org/10.1042/BSR20170082.

Wei, Y.H., Wang, L.F., Chang, J.S., 2004. Optimizing iron supplement strategies for enhanced surfactin production with *Bacillus subtilis*. Biotechnol. Prog. 20 (3), 979–983. https://doi.org/10.1021/bp030051a.

Weinberg, E.D., 1969. Biosynthesis of secondary metabolites: roles of trace metals. Adv. Microb. Physiol. 4, 1–44.

Weinberg, E.D., 1990. Roles of trace metals in transcriptional control of microbial secondary metabolism. Biol. Met. 2 (4), 191–196.

Wewetzer, S.J., Kunze, M., Ladner, T., Luchterhand, B., Roth, S., Rahmen, N., Kloss, R., Costa, E.S.A., Regestein, L., Büchs, J., 2015. Parallel use of shake flask and microtiter plate online measuring devices (RAMOS and BioLector) reduces the number of experiments in laboratory-scale stirred tank bioreactors. J. Biol. Eng. 9, 9. https://doi.org/10.1186/s13036-015-0005-0.

WHO, 2017. Prioritization of Pathogens to Guide Discovery, Research and Development of New Antibiotics for Drug-Resistant Bacterial Infections, Including Tuberculosis ((WHO/EMP/IAU/2017.12)). Retrieved from Geneva: https://www.who.int/medicines/publications/global-priority-list-antibiotic-resistant-bacteria/en/.

Yang, W., Yang, X., 2010. Molecular dynamics study of the influence of calcium ions on foam stability. J. Phys. Chem. B 114 (31), 10066–10074. https://doi.org/10.1021/jp1022828.

Yao, S., Zhao, S., Lu, Z., Gao, Y., Lv, F., Bie, X., 2015. Control of agitation and aeration rates in the production of surfactin in foam overflowing fed-batch culture with industrial fermentation. Rev. Argent. Microbiol. 47 (4), 344–349. https://doi.org/10.1016/j.ram.2015.09.003.